Determination of microscopic parameters for nonresonant energy-transfer processes in rare-earth-doped crystals

L. V. G. Tarelho, L. Gomes,* and I. M. Ranieri
Instituto de Pesquisas Energéticas e Nucleares, Comissão Nacional de Energia Nuclear, Caixa Postal 11049, Pinheiros, 05422-970, Brazil
(Received 21 August 1996; revised manuscript received 28 May 1997)

A method for estimating the microscopic probability rate of phonon-assisted energy transfer between rare-earth $(3+)$ ions in solids was developed based on Dexter's theory for phonon-assisted energy transfer. The proposed method in this paper enables one to calculate the overlap integral from fundamental cross-section spectra of nonresonant energy transfer involving a multiphonon generation in both donor and acceptor sites. A translation of the donor emission spectrum towards the acceptor absorption scaled with the N-phonon emission probability represents the m-phonon emission band which performs the energy transfer to the acceptor. A nonvanishing overlap integral $10^{-2}-10^{-3}$ times smaller than for the resonant case is found. A multiphonon generation probability assisting the energy transfer was considered due to a combined mechanism of creation and annihilation of phonons. The participation of each phonon in the process was determined. This method was used to investigate the $Tm^{3+}(^3F_4)\rightarrow Ho^{3+}(^5I_7), Er^{3+}(^4I_{13/2})\rightarrow[Ho^{3+}(^5I_7), Tm^{3+}(^3F_4)]$ direct energy transfers in $LiYF_4$ crystals, as well the back transfers.
[S0163-1829(97)00545-6]

I. INTRODUCTION

Förster and Dexter developed the basic theory of sensitized luminescence in solids based on the ion-ion interactions produced by electric multipole effects.[1,2] The evaluation of the energy-transfer probability is related to the overlap integral between donor emission and acceptor absorption cross-section spectra. Kushida in 1973 applied that method for several processes involving interactions between $(3+)$ rare-earth ions in crystals, such as resonant energy transfer, cooperative excitation transfer, and cooperative optical transitions.[3] In 1992, Payne and co-workers evaluated the critical radii of resonant energy-transfer processes for Tm^{3+} $(^3F_4)$ and Ho^{3+} $(^5I_7)$ in $LiYF_4$ crystals,[4] confirming the usefulness of this method.

Nevertheless, energy transfer can occur for cases where an energy mismatch is found to be much larger than the cutoff lattice phonon energy. This nonresonant process can be assisted by local phonons and the energy difference ΔE must be given to the lattice vibrations. The interaction must contain an electron-phonon component.[5] The initial and final states must include the initial and final phonon states, which will differ by a number of phonons whose total energy is ΔE. If ΔE is larger than the phonon energy $(\hbar\omega_0)$, more than one phonon will be created in the donor $(D)\rightarrow$ acceptor (A) process or destroyed in the reverse $A\rightarrow D$ process. Miyakawa and Dexter[5] treated this problem and verified that it is also legitimate to write the expression for the probability rate of energy transfer in the form

$$W_{D-A}=\left(\frac{2\pi}{\hbar}\right)|H_{DA}|^2 S_{DA}^N, \tag{1}$$

where S_{DA}^N is the overlap integral between the m-phonon emission line shape of ion D (m-phonon emission sideband) and the k-phonon absorption line shape of ion A (k-phonon absorption sideband). For the case of small electron-phonon coupling (i.e., S_0^D and $S_0^A<1$) S_{DA}^N can be approximated by[5]

$$S_{DA}^N \approx \sum_N e^{-(S_0^D+S_0^A)}\left[\frac{(S_0^D S_0^A)^N}{N!}\right] S_{DA}(0,0,E)\,\partial(N,\Delta E/\hbar\omega_0), \tag{2}$$

where $S_{DA}(0,0,E)$ represents the overlap integral between the zero-phonon lines shape of donor emission and absorption of acceptor ions. This zero-phonon overlap should be produced for some hypothetical host system with an energy match, i.e., $\Delta E=0$. One must note that $S_{DA}(0,0,E)$ vanishes for an energy mismatch $\Delta E>\hbar\omega_0$. Using the results expressed by Eqs. (1) and (2), Dexter also derived an energy gap law for the energy-transfer probability[5]

$$W_{D-A}(\Delta E)=W_{D-A}(0)\exp(-\beta\Delta E). \tag{3}$$

β is the temperature-dependent parameter and is related to the analogous parameter in a similar law for the dependence on the energy gap to the next lower level of nonradiative decay rate of a state by multiphonon emission. Equation (3) depends exponentially on the energy gap in the same way as the multiphonon relaxation probability. This dependence is confirmed experimentally for the multiphonon relaxation processes[6] and may be used to estimate the transfer probability between ions with different excitation energies.

In spite of all the developments made to understand the nonresonant energy-transfer process between rare-earth ions in solids, an accessible method to determine the microscopic parameters of interaction from experimental spectra is still missing. Several barriers to the calculation of the critical radius for a nonresonant energy transfer in solids are found in Dexter's formulas. For example, the result expressed by Eq. (1) implies the use of both sidebands, i.e., the m-phonon emission band of the donor (ion D) and the k-phonon ab-

sorption of the acceptor (ion A). Generally these sidebands are very weak, about 10^{-2}–10^{-3} times smaller than the zero-phonon band, when two or more phonons are involved in the process (i.e., $m \geqslant 2$ and $k \geqslant 2$). The detectability of the m-phonon emission sideband for $m \geqslant 2$ is very much limited by the signal-to-noise ratio which is, in fact, very poor for transitions located in the near- and middle-infrared region where the most important energy-transfer processes take place. Besides this, one-phonon sidebands have been experimentally found in the excitation spectra of anti-Stokes excitation of $Er^{3+}(^4S_{3/2})$ and Stokes emission of $Ho^{3+}(^5F_5)$ in CdF_3, WO_4Ca, LaF_3, and HoF_3 crystals.[7]

On the other hand, the energy gap law [Eq. (3)] can be used to estimate $W_{DA}(0)$ if one could estimate parameters β and ΔE by independents ways. The critical radius of interaction can be obtained from the $W_{D-A}(0)$ estimate, however, this would be dependent on the statistics used to correlate the microscopic probability rate with the macroscopic rate $(1/\tau)$ obtained from the lifetime measurement (τ). In addition, the energy gap law expressed by Eq. (3) only gives a mean description of the phonon process which has, in fact, an average order equal to $N = \Delta E/\hbar\omega_0$. This exponential relation has been used to calculate the multiphonon absorption cross sections of Er^{3+} between $^4I_{9/2}$ and $^4S_{3/2}$ terms in order to explore the link between the photon avalanche initial step and the multiphonon sideband absorption in the $LiYF_4$ crystal.[8]

In this paper we propose a method that allows one to calculate the important microscopic parameters of interaction (i.e., critical radius (R_C) and transfer constant $[C_{D-A}$ or C_{A-D} $(\mathrm{cm}^6/\mathrm{s})]$ based on the actual theory of phonon-assisted energy transfer. These microscopic parameters can be obtained directly from the overlap integral between the zero-phonon emission and absorption cross sections of donor and acceptor ions. This was done just using Dexter's result which correlates the overlap integral between phonon sidebands with the overlap integral between the respective zero-phonon bands of ions D and A.

The transfer probability rate derived from the proposed model depends on both the nonvanishing overlap integral due to the translation of the donor emission spectrum towards the acceptor absorption, and the adimensional probability of multiphonon generation due to a creation (emission) and annihilation (absorption) of phonons. These phonon processes mainly occur in the donor site. This method is used to calculate the critical radii of resonant, quasiresonant, and nonresonant energy-transfer processes involving the first excited states of Er^{3+}, Tm^{3+}, and Ho^{3+} in $LiYF_4$ crystals.

II. DETERMINATION OF THE MICROSCOPIC PARAMETERS FOR NONRESONANT ENERGY TRANSFER: AN EXTENDED APPROACH OF THE OVERLAP INTEGRAL METHOD

The microscopic energy-transfer probability rate between donor and acceptor ions considering a dipole-dipole interaction was described by Dexter[2]

$$W_{D-A}(R) = \frac{C_{D-A}}{R^6}, \tag{4}$$

where R is the distance of separation between donor and acceptor, and C_{D-A} is the transfer constant $(\mathrm{cm}^6/\mathrm{s})$ defined as follows:

$$C_{D-A} = \frac{R_C^6}{\tau_D}$$

R_C is the critical radius of the interaction and τ_D the intracenter lifetime of the donor excited level. R_C is given by

$$R_C^6 = \frac{6c\tau_D}{(2\pi)^4 n^2} \frac{g_{\mathrm{low}}^D}{g_{\mathrm{up}}^D} \int \sigma_{\mathrm{emis}}^D(\lambda)\sigma_{\mathrm{abs}}^A(\lambda)\,d\lambda, \tag{5}$$

where n is the refractive index of medium, c is the speed of light and $\sigma_{\mathrm{abs}}^A(\lambda)$ and $\sigma_{\mathrm{emis}}^D(\lambda)$ are the absorption (acceptor) and emission (donor) cross-section spectra. g_{low}^D and g_{up}^D are the degeneracies of donor (D) states, respectively, from the lower and upper levels involved in the process. It is convenient to define the overlap integral exhibited in Eq. (5) as

$$S_{DA}(\lambda) = \int \sigma_{\mathrm{emis}}^D(\lambda)\sigma_{\mathrm{abs}}^A(\lambda)\,d\lambda.$$

A nonvanishing overlap integral [i.e., $S_{DA}(\lambda) \neq 0$] between both cross-section spectra is a characteristic of resonant and quasiresonant processes of nonradiative energy transfer between $(3+)$ rare-earth ions in solids.

In the case of rare-earth ion interaction, the emission cross-section spectrum of a donor level can be obtained from the respective absorption spectrum using the McCumber relation[9] as follows:

$$\sigma_{\mathrm{emis}}(\lambda) = \sigma_{\mathrm{abs}}(\lambda)\,\frac{N_1}{N_2}\,\exp\left(\frac{-\hbar\omega}{k_B T}\right). \tag{6}$$

$\hbar\omega$ is the energy related to the absorption wavelength λ. N_1/N_2 is the population ratio between donor levels verified in the equilibrium temperature T. N_1 and N_2 are the ground- and excited-state populations of the donor, respectively obtained using the Boltzmann distribution applied to the manifold Stark levels of each considered multiplet. N_1 and N_2 were obtained using

$$N_1 = \sum_i g_i \exp(-E_i/k_B T),$$

$$N_2 = \sum_j g_j \exp(-E_j/k_B T),$$

where g_i and g_j represent the sublevel degeneracies, i.e., (i) for ground state and (j) for excited state. Equation (6) is valid for an ion system where the Huang-Rhys factor is small, i.e., $S_0 < 1$, or for a small Stoke's shift between absorption and emission. This condition is well satisfied by $(3+)$ rare-earth-ion transitions in solids $(S_0 \cong 0.31)$.[10]

The nonresonant energy transfer between donor and acceptor ions was treated by Miyakawa and Dexter,[5] where they concluded that the overlap integral of Eq. (1) can be written as a sum of each overlap integral involving emission and absorption sidebands. However, one must pay attention to Dexter's result about the overlap integral between the

phonon sidebands for the case of small electron-phonon coupling ($S_0<1$). In this case, they determined that

$$S_{D-A}(m,k,E)\approx\frac{S_0^m S_0^k}{m!k!}\,e^{-2S_0}S_{D-A}(0,0,E), \tag{7}$$

$$S_{D-A}(0,0,E)=\int g^D_{\rm emis}(E)g^A_{\rm abs}(E)dE.$$

$S_{D-A}(0,0,E)\approx 0$ in the case of nonresonant energy transfer, unless one takes the zero-phonon line shape of donor emission as $g^D_{\rm emis}(E-\Delta E)$ with $\Delta E=$ energy mismatch. Working out Eq. (7) for the case of m-phonon emission by the donor and no-phonon involvement by the acceptor, one has

$$\begin{aligned}S_{D-A}(m,0,E)&=\int g^D_{\rm emis(\,m-phonon)}(E)g^A_{\rm abs}(E)dE\\&=\frac{S_0^m}{m!}\,e^{-S_0}S_{D-A}(0,0,E)\\&=\int\left(\frac{S_0^m}{m!}\,e^{-S_0}g^D_{\rm emis}(E-\Delta E)\right)g^A_{\rm abs}(E)dE,\end{aligned}$$

where $\Delta E=m\hbar\omega_0$. Considering the fact that both the zero-phonon emission line shape and the m-phonon emission sideband have approximately the same width, one finds a general result as the m-phonon emission line shape (emission sideband) of ion D can be obtained from the measured zero-phonon emission band if properly scaled using the m-phonon emission probability and the proper energy translation by $m\hbar\omega_0$. Of course, this multiphonon probability must include both the spontaneous and estimulated $(\overline{n}+1)$ terms for the system at some finite temperature T. The following relations are therefore proposed for the spectral sideband calculations from the measured emission and absorption intermultiplet transitions for $RE(3+)$ ions

$$\sigma^D_{\rm emis(\,m-phonon)}\approx\frac{S_0^m e^{-S_0}}{m!}\,(\overline{n}+1)^m\sigma^D_{\rm emis(expt)}(E-E_1), \tag{8}$$

$$\sigma^A_{\rm abs(\,k-phonons)}\cong\frac{S_0^k e^{-S_0}}{k!}\,(\overline{n})^k\sigma^A_{\rm abs(expt)}(E+E_2), \tag{9}$$

where $E_1=m\hbar\omega_0$, $E_2=k\hbar\omega_0$, and $\Delta E=E_1+E_2$. An overestimate of the overlap integral is obtained when using the experimental emission band in Eq. (8) due to the contribution of one-phonon emission to the experimental emission spectrum. This contribution is estimated to be about 22% of the zero-phonon emission band for $RE(3+)$ in $LiYF_4$ crystals at 300 K. Spectral separation of this one-phonon emission contribution would be impossible to do because the complexity of the emission spectrum which has a superposition of tens of zero-phonon lines. However in the case of absorption transition, the contribution of the one-phonon sideband is negligible (10^{-2}). This suggests that the best determination of the emission sideband of a donor [from Eq. (8)] would be one which uses the emission cross section calculated by the McCumber method. This procedure minimizes the intrinsic error in the emission sideband determination considering that the absorption spectra only has zero-phonon lines contributions.

A composition of the translation of the emission spectrum of the donor towards the acceptor absorption by E_1 and vice versa in the case of acceptor absorption enables one to calculate the overlap integral $S_{D\text{-}A}(m,k,E)$ using experimental emission and absorption cross-section spectra. The translation of the emission spectrum by $(m\hbar\omega_0)$ and the absorption spectrum by $(k\hbar\omega_0)$ should be performed in order to simulate the sideband overlap. Each overlap contribution, involving a combination of creation and annihilation of phonons in both donor and acceptor sites, must be computed for each case of energy conservation where $\Delta E=(m+k)\hbar\omega_0$.

Another important fact is that the two multiphonon processes occurring in both donor and acceptor sites cannot completely describe the energy transfer in a system at equilibrium temperature T. Three dependent multiphonon processes would be necessary to assist the energy transfer. Only one multiphonon process involving m-phonon emission must occur in the donor site. However, two multiphonon processes have to occur in the acceptor site, i.e., k-phonon absorption followed by k-phonon emission. The acceptor must emit k phonons after receiving the donor's excitation in order to reach their lowest excited state (the zero-phonon Stark level) which is the most populated state at equilibrium temperature T. Figure 1 shows a schematic diagram of the energy levels involved exhibiting the proposed three multiphonon processes necessary to assist the energy transfer for the nonresonant case. As illustrated in Fig. 1(a), $(N\text{-}k)$ phonons can be emitted by the donor while k phonons are absorbed by the acceptor in the case of $D\rightarrow A$ transfer. This mechanism matches both the energy levels of donor and acceptor propiciating conditions for a ''resonant-type'' transfer. The total probability of phonon generation must take into account that at the end of the process, the acceptor has to emit k phonons in order to reach its zero-phonon excited state. Figure 1(b) indicates the three multiphonon processes necessary to assist the $(A\rightarrow D)$ back transfer.

The probability of the three-multiphonon process (or N-phonon generation) for each case, is given (a) for direct transfer $(D\rightarrow A)$

$$[P^+_{(N-k)}\cdot P^-_k\cdot P^+_k],$$

(b) for back transfer $(A\rightarrow D)$

$$[P^-_{(N-k)}\cdot P^+_k\cdot P^-_k].$$

The signal $(+)$ was used to specify the phonon creation probability and $(-)$ for the phonon annihilation.

By this consideration, the microscopic probability rate based on the evaluation of the overlap integral between the absorption and emission cross sections can be obtained using the following equations valid for direct transfer:

$$\begin{aligned}W_{DA}(R)=&\frac{6cg^D_{\rm low}}{(2\pi)^4n^2R^6g^D_{\rm up}}\sum_{N=0}^{\infty}\sum_{k=0}^{N}P^+_{(N-k)}P^-_kP^+_k\\&\times\int\sigma^D_{\rm emis}(\lambda^+_{(N-k)})\sigma^A_{\rm abs}(\lambda^-_k)d\lambda,\end{aligned} \tag{10}$$

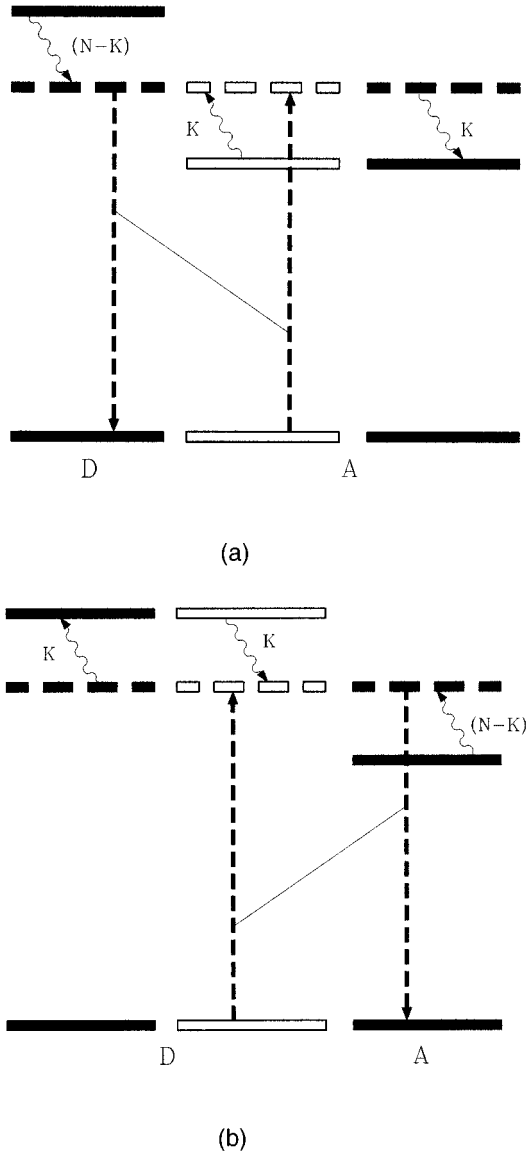

FIG. 1. Schematic diagram showing the three multiphonon processes necessary to completely assist the nonresonant energy transfer between donor and acceptor ions. (a) shows the direct $D \rightarrow A$ transfer where $(N-k)$ phonons are created in the donor site, while k phonons are annihilated by the acceptor. Broken lines represent a virtual intermediate excited state from where the excited energy is resonantly transferred to the acceptor. In the next step, the acceptor had to emit k phonons in order to reach the zero-phonon state which is the most populated state in the system at equilibrium temperature T. The total probability of phonon generation is given by $[P^{+}_{(N-k)}P^{-}_{k}P^{+}_{k}]$. (b) shows all the three multiphonon processes necessary to assist the back transfer $(A \rightarrow D)$. In this case, the total probability of phonon generation is given by $[P^{-}_{(N-k)}P^{+}_{k}P^{-}_{k}]$.

where

$$\sum_{k=0}^{N} P^{+}_{(N-k)}P^{-}_{k}P^{+}_{k}\int \sigma^{D}_{\mathrm{emis}}(\lambda^{+}_{(N-k)})\sigma^{A}_{\mathrm{abs}}(\lambda^{-}_{k})d\lambda \cong\left(\sum_{k=0}^{N} P^{+}_{(N-k)}P^{-}_{k}P^{+}_{k}\right)\int \sigma^{D}_{\mathrm{emis}}(\lambda^{+}_{N})\sigma^{A}_{\mathrm{abs}}(\lambda)d\lambda.$$

Here $\sigma^{D}_{\mathrm{emis}}$ and $\sigma^{A}_{\mathrm{abs}}$ represent the cross-section spectra experimentally measured. It is recommended to use the emission cross section obtained from the use of the McCumber method. $\lambda^{+}_{(N-k)}$ denotes the translation of the emission cross-section wavelength by $(N-k)$-phonon emission by the donor. λ^{-}_{k} represents the translation of the absorption cross-section spectra wavelength of the acceptor due to k-phonon absorption (or annihilation)

$$\lambda^{+}_{(N-k)}=\frac{1}{1/\lambda-(N-k)\hbar\omega_0},$$

$$\lambda^{-}_{k}=\frac{1}{1/\lambda+k\hbar\omega_0}.$$

$P^{+}_{(N-k)}$ is the probability of $(N-k)$-phonon emission by the donor and P^{-}_{k} denotes the probability of k-phonon absorption by the acceptor, necessary to assist the energy transfer. These probabilities can be derived from the multiphonon decay rate described by a nonadiabatic process for systems where the Stoke's shift (or the Huang Rhys factor S_0) is not zero.[11] The following equation proceeds in that case for a process where N phonons of average energy $\hbar\omega_0$ are created:[10]

$$W_{nr}=W_0\ \exp\left(-S_0\,\frac{1+r}{1-r}\right)\times\sum_{j=0}^{\infty}\frac{\{S_0[r/(1-r)]\}^{j}\{S_0[1/(1-r)]\}^{N+j}}{j!(N+j)!}. \quad (11)$$

W_0 is the attempt frequency of phonon-emission stimulation which is of the order of $10^{13}\ \mathrm{s}^{-1}$, and $r=\exp(-\hbar\omega_0/k_BT)$. ω_0 is the effective phonon frequency. It is interesting to note that the sum in Eq. (11) represents all the possibilities of $(N+j)$-phonon creation followed by j-phonon annihilation. By the inspection of Eq. (11) we concluded that only the first term $(j=0)$ gives an important contribution for rare-earth ions. Based on this argument, we define that both probabilities of creation of $(N-k)$ and annihilation of k phonons are obtained by the ratio (W_{nr}/W_0) given by

$$P^{+}_{(N-k)}\cong\exp[-(2\overline{n}+1)S_0]\,\frac{S_0^{(N-k)}}{(N-k)!}\,(\overline{n}+1)^{(N-k)},$$

$$P^{-}_{k}\cong\exp[-2\overline{n}S_0]\,\frac{S_0^{k}}{k!}\,(\overline{n})^{k},$$

where $\overline{n}=1/(e^{(\hbar\omega_0/KT)}-1)$ is the average occupancy of phonon mode at temperature T.

The critical radius of the interaction can be derived using Eqs. (4) and (10) given (a) for $(D \rightarrow A)$ direct transfer

$$R_C^6=\frac{6c\tau_D g^{D}_{\mathrm{low}}}{(2\pi)^4 n^2 g^{D}_{\mathrm{up}}}\sum_{N=0}^{\infty}\int \sigma^{D}_{\mathrm{emis}}(\lambda^{+}_{N})\sigma^{A}_{\mathrm{abs}}(\lambda)d\lambda\times\left(\sum_{k=0}^{N} P^{+}_{(N-k)}P^{-}_{k}P^{+}_{k}\right), \quad (12)$$

(b) for the $(A \rightarrow D)$ back transfer

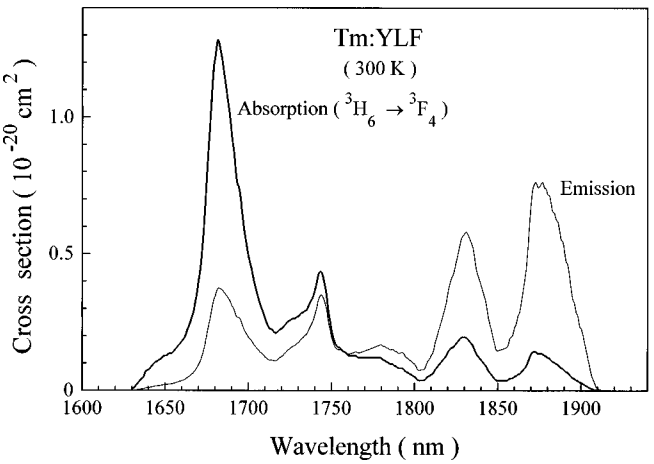

FIG. 2. Spectral cross-section superposition between the fundamental $^3H_6 \rightarrow {}^3F_4$ absorption and $^3F_4 \rightarrow {}^3H_6$ emission of Tm(3+) ions in YLF crystals (at 300 K). From that, the overlap integral was obtained and the critical radius (R_C) for the energy migration through $^3F_4$ states determined.

$$R_C^6 = \frac{6c\tau_A g_{\text{low}}^A}{(2\pi)^4 n^2 g_{\text{up}}^A} \sum_{N=0}^{\infty} \int \sigma_{\text{emis}}^A(\lambda_N^-)\sigma_{\text{abs}}^D(\lambda)d\lambda \times \left(\sum_{k=0}^{N} P_{(N-k)}^- P_k^+ P_k^- \right). \quad (13)$$

Equations (12) and (13) are essentially obtained in our proposed method in this paper. This allows one to calculate the microscopic parameters (R_C and C_{D-A}) for the nonresonant (phonon-assisted) energy transfer, directly from the experimental cross-section spectra. This result constitutes an upgrade of the overlap integral method which has been largely used to calculate the microscopic parameters only for resonant and quasiresonant energy transfers.

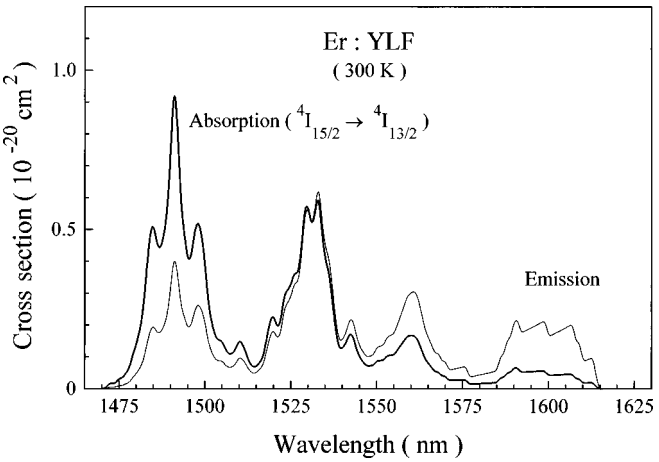

FIG. 3. This figure shows the spectral cross-section superposition between the fundamental $^4I_{15/2} \rightarrow {}^4I_{13/2}$ absorption and $^4I_{13/2} \rightarrow {}^4I_{15/2}$ emission of Er(3+) ions in YLF crystals at 300 K. From that, the overlap integral was obtained and the critical radius (R_C) for the energy migration through the $^4I_{13/2}$ states determined.

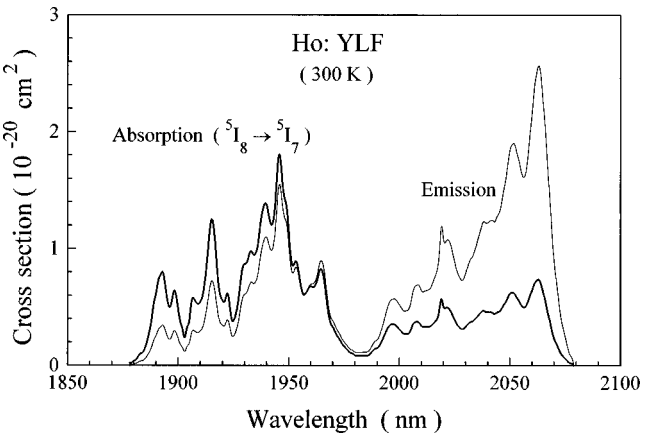

FIG. 4. This figure shows the spectral cross-section superposition between the fundamental $^5I_8 \rightarrow {}^5I_7$ absorption and $^5I_7 \rightarrow {}^5I_8$ emission of Ho(3+) ions in YLF crystals at 300 K. From that, the overlap integral was obtained and the critical radius (R_C) for the energy migration through the $^5I_7$ states determined.

III. MICROSCOPIC PARAMETERS OF ENERGY TRANSFER BETWEEN Er^{3+}, Tm^{3+}, AND Ho^{3+} IONS IN $LiYF_4$ CRYSTALS

Ho, Er, and Tm(3+) doped $LiYF_4$ (YLF) crystals have been used in this work to verify the usefulness of the present method and to give a microscopic description of the ion-ion energy transfer in holmium-doped laser crystals. The critical radius of both direct and back-transfer processes for Tm-Er and Er-Ho were obtained in this paper. The direct transfers studied were from $^4I_{13/2}$(Er) and $^3F_4$(Tm) donor levels to the $^7I_7$(Ho) acceptor level. Figures 2–4 show the absorption and emission cross sections for the optical transitions involving the ground and the first excited states of these ions. The absorption cross sections were obtained from the absorbance spectra of oriented crystals having the c axis in the plane perpendicular to the light propagation vector in the medium. This makes the absorption spectra free of polarization effects. The emission cross-section spectra were obtained from the absorption using Eq. (6). The ions concentrations were determined by x-ray fluorescence analysis and the results are listed in Table I.

Using the data of Figs. 2–4 in Eq. (5), the critical radii of resonant (Tm→Tm), (Er→Er), and (Ho→Ho) energy transfers and the respective C_{D-D} have been calculated. The obtained values are given in Table II.

The critical radius of the nonresonant (Tm→Ho, Er→Tm, Er→Ho) energy transfers was evaluated using the relation given in Eq. (12). The Nth term of the overlap integral was obtained from the spectral cross-section superposi-

TABLE I. Measured ion concentrations (mol %) and the lifetimes (τ_D) measured at 300 K for the first excited states of (3+) rare-earth-doped YLF crystals.

Ion (mol %)	Level	τ_D (ms)
Er (1)	$^4I_{13/2}$	11
Tm (0.73)	$^3F_4$	14.5
Ho (1.71)	$^5I_7$	15.2

TABLE II. Critical radii (R_C) and $C_{D\text{-}D}$ (cm^6/s) constants obtained using Eqs. (2) and (3) for the Tm→Tm, Er→Er, and Ho→Ho resonant energy transfers, involving the ground and the first excited states of these ions.

Energy migration (resonant)	$C_{D\text{-}D}$ (10^{-40} cm^6/s)	R_C (Å)
$Ho(^5I_7)\rightarrow Ho(^5I_7)$	522(78)	30(1)
$Tm(^3F_4)\rightarrow Tm(^3F_4)$	124(20)	23.7(1)
$Er(^4I_{13/2})\rightarrow Er(^4I_{13/2})$	41(6)	18.9(1)

tion between the donor emission (redshifted by m phonons) and the acceptor absorption (blueshifted by k phonons). Figures 5–7 give some particular energy matched N-phonon sidebands, in order to illustrate how this method works. For the cases of pure nonresonant transfers, i.e., Er→Tm, Er→Ho, the overlap integrals $S_{DA}(\lambda)$ are zero and consequently one will have $S^N_{DA}(\lambda^+_N,\lambda)\neq 0$ for each case after a proper translation of the donor emission spectrum by $N\hbar\omega_0$ energy according to

$$\lambda^+_N=\frac{1}{1/\lambda-N\hbar\omega_0}$$

[where $\hbar\omega_0\cong 331\ cm^{-1}$ for YLF (Refs. 6 and 10)].

It is observed that $S^N_{DA}(\lambda^+_N,\lambda)$ increases with the number of emitted phonons (N) in the donor site. On the other hand, the probability term P^+_N decreases as N increases. According to Eq. (10), the rate probability of the Nth term depends on the product of both terms, i.e., $[S^N_{DA}(\lambda^+_N,\lambda)\Sigma_k P^+_{(N-k)}P^-_k P^+_k]$. The contribution of a particular $[(N-k),k]$th term of the probability rate can be estimated using the quantities R_1 and R_2 defined as

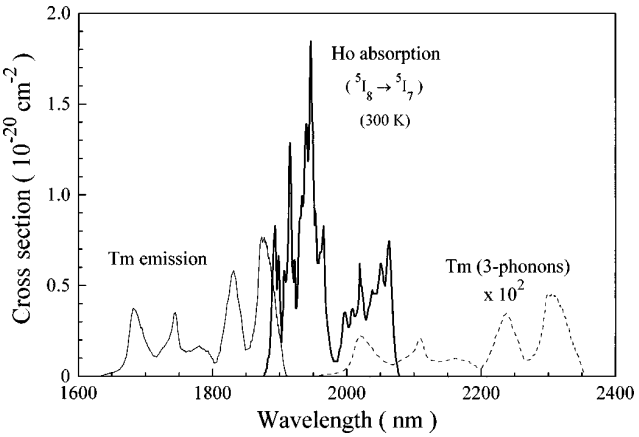

FIG. 5. Spectral cross-section superposition between the $^3F_4\rightarrow{}^3H_6$ emission of Tm(3+) (solid line) and the fundamental $^5I_8\rightarrow{}^5I_7$ absorption of Ho(3+) ions (dark solid line) in YLF crystals at 300 K. The emission sideband of Tm involving three phonons, in the donor site ($m=3$, $k=0$), was calculated using Eq. (8). It is represented by the broken line. Other nonvanishing overlap integrals were also obtained due to one- and two-phonon emission by Tm ions (not shown). The only exhibited energy-matched multiphonon sideband of Tm(3+) ($m=3$ and $k=0$) is shown as an example.

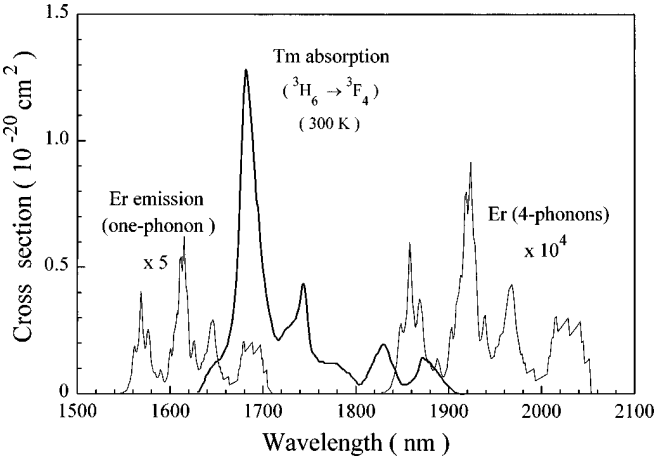

FIG. 6. Spectral superposition between the cross sections of the one-phonon emission sideband of $^4I_{13/2}\rightarrow{}^4I_{15/2}$ zero-phonon emission of Er(3+) (solid line) and the $^3H_6\rightarrow{}^3F_4$ absorption of Tm(3+) ions (dark solid line) in YLF crystals at 300 K. The four-phonon emission sideband of $^4I_{13/2}\rightarrow{}^4I_{15/2}$ of Er(3+) is represented on the right side. Other nonvanishing overlap integrals were also obtained due to two- and three-phonon emission sidebands of the Er ion (not shown). The one-phonon and four-phonon Er sidebands were calculated from Eq. (8) using ($m=1$, $k=0$) and ($m=4$, $k=0$), respectively.

$$R_1=\frac{S^N_{DA}(\lambda^+_N,\lambda)P^+_{(N-k)}P^-_k P^+_k}{\Sigma^\infty_{N=0}S^N_{DA}(\lambda^+_N,\lambda)\Sigma^N_{k=0}P^+_{(N-k)}P^-_k P^+_k}$$

for direct transfer and

$$R_2=\frac{S^N_{AD}(\lambda^-_N,\lambda)P^-_{(N-k)}P^+_k P^-_k}{\Sigma^\infty_{N=0}S^N_{AD}(\lambda^-_N,\lambda)\Sigma^N_{k=0}P^-_{(N-k)}P^+_k P^-_k}$$

for back transfer.

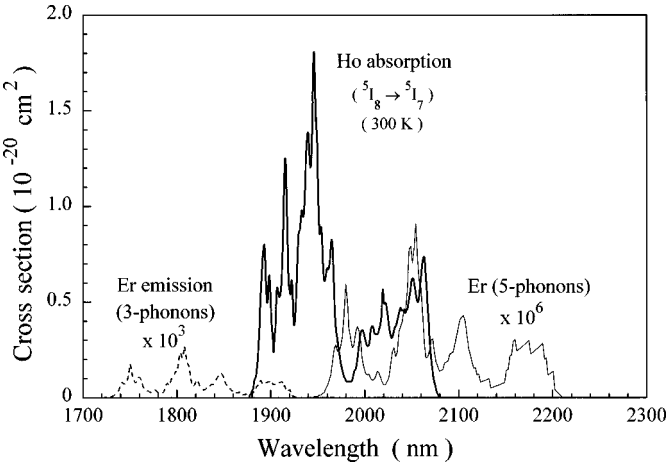

FIG. 7. Spectral superposition between the cross sections of the three-phonon emission sideband of $^4I_{13/2}\rightarrow{}^4I_{15/2}$ zero-phonon emission of Er(3+) (dashed line) and the fundamental $^5I_8\rightarrow{}^5I_7$ absorption of Ho(3+) (dark solid line) in YLF crystals at 300 K. The five-phonon emission sideband of the $^4I_{13/2}\rightarrow{}^4I_{15/2}$ transition of Er(3+) is represented on the right side (solid line). Another nonvanishing overlap integral was also obtained with the four-phonon emission sideband of Er (not shown). These three-phonon and five-phonon Er sidebands were calculated from Eq. (8) using ($m=3$, $k=0$) and ($m=5$, $k=0$), respectively.

TABLE III. Critical radii (R_C) and $C_{D\text{-}A}$ (cm^6/s) constants obtained using Eqs. (8) and (9) for Tm→Ho, Er→Tm, and Er→Ho direct transfers (a) as well as for the back transfers (b). The number (#) of phonons necessary to assist the energy transfer as well as the percentage of each phonon participation (%) in the process, are indicated.

Nonresonant $D \rightarrow A$	N (# of phonons) (% phonon-assist.)	$C_{D\text{-}A}$ (10^{-40} cm^6/s)	R_C (Å)
(Direct transfer)	[a]		
$Tm(^3F_4) \rightarrow Ho(^5I_7)$	0,1,2 (68;26.2;5.8%)	51.6(8)	20.5(1)
$Er(^4I_{13/2}) \rightarrow Tm(^3F_4)$	1,2,3 (72.6;24.1;3.3%)	10.3(2)	15.0(1)
$Er(^4I_{13/2}) \rightarrow Ho(^5I_7)$	3,4,5 (68;30.6;1.4%)	0.27(1)	8.2(1)
(Back transfer)	[b]		
$Ho(^5I_7) \rightarrow Tm(^3F_4)$	0,1,2 (69.2;28;2.7%)	15.6(2)	16.9(1)
$Tm(^3F_4) \rightarrow Er(^4I_{13/2})$	1,2,3,4 (34;12;52;2%)	0.01(1)	4.9(1)
$Ho(^5I_7) \rightarrow Er(^4I_{13/2})$	3,4,5 (67.6;31;1.4%)	0.0004(1)	2.9(1)

[a]Phonon emission.
[b]Phonon annihilation.

Table III shows the N-phonon contribution term (%) to the total probability rate of the energy transfer. The respective critical radii and C_{D-A} constants are also given in Table III. The (Tm→Er) and (Ho→Er) back transfers were also analyzed for the interaction involving the first excited state of the donor and the ground state of the acceptor. The result shows that the direct (Er→Ho) transfer needs the assistance of 3 (68.2%), 4 (30.4%), and 5 (1.4%) phonon emissions in the Er site while the respective back transfer needs the assistance of 3 (67.6%), 4 (31%), and 5 (1.4%) phonon absorptions (or annihilations). Both the direct Tm→Ho transfer and the respective back transfer, which are known to be quasiresonant processes, have a participation of 1 and 2 phonons for each process. It was also verified that the Tm→Ho transfer has the assistance of one-phonon (26.2%) and two-phonon (5.8%) processes. It means that the zero-phonon participates only with 68% of the total process.

IV. DISCUSSION

Comparing the obtained C_{D-A} values for the energy transfers involving Er, Tm, and Ho ions in $LiYF_4$ crystals at 300 K, one finds that the resonant $^3F_4(\mathrm{Tm}) \rightarrow {}^5I_7(\mathrm{Ho})$ transfer is the most probable microscopic process to occur in contrast with the nonresonant $^4I_{13/2}(\mathrm{Er}) \rightarrow {}^5I_7(\mathrm{Ho})$ transfer. The obvious conclusion is that a nonresonant phonon-assisted energy transfer involving several-phonon generation must always be less probable to occur than the resonant process. The obtained R_C values also reinforce this fact.

It was also observed that the $^4I_{13/2}(\mathrm{Er}) \rightarrow {}^3F_4(\mathrm{Tm})$ microscopic energy transfer is more effective than the $^4I_{13/2}(\mathrm{Er}) \rightarrow {}^5I_7(\mathrm{Ho})$ (38 times higher), besides the fact that both are nonresonant processes. For the case of Er→Tm transfer we observed a multiphonon mechanism dominated by the one-phonon creation (72.6%), while for Er→Ho transfer three- (68.2%) and four-phonon (30.4%) creations are involved.

Another important point to emphasize is the effectiveness of the back-transfer mechanism (Ho→Tm) compared with direct transfer. In general, back transfer is always less probable than direct-transfer process. It was seen for the case of (Er→Tm) and (Er→Ho) transfers, the back-transfer probability is $\leqslant 1.5\times 10^{-1}\%$ of the direct process. On the other hand, the (Ho→Tm) back transfer represents 30% of the direct (Tm→Ho) transfer.

Our calculated critical radii (1) $R_C = 30$ Å for Ho→Ho transfer, (2) $R_C = 23.7$ Å for Tm→Tm transfer, (3) $R_C = 20.5$ Å for Tm→Ho transfer, and (4) $R_C = 16.9$ Å for Ho→Tm back transfer (all obtained from unpolarized cross-section measurements) agree well with the values of Ref. 4 assuming that $R_C = [R_\sigma^2 + R_\pi^2]^{1/2}$. The following R_C values were derived from Ref. 4 for comparison: (1) 32 Å, (2) 29.2 Å, (3) 23.5 Å, and (4) 17.8 Å. In that case they estimated R_σ and R_π from the σ and π polarized cross-section measurements in YLF crystals. Of course, for a precise critical radius determination one must use the unpolarized overlap integral spectra. Underestimated R_C values can be obtained from the overlap integral method when one uses the polarized cross-section spectra in the calculation.

A complete description of microscopic interactions between $RE(3+)$ ions must take into account both probability rates of direct- and back-transfer processes. For this purpose we define an effective microscopic probability rate for the energy transfer defined as follows:

$$W_{D-A}^{ef} = W_{D-A} - W_{A-D} \Rightarrow C_{D-A}^{ef} = C_{D-A} - C_{A-D}\,.$$

The effective critical radius for Tm→Ho transfer, using the estimated C_{D-A}^{ef} constant, was calculated. The following values were obtained for Tm→Ho transfer: $C_{D-A}^{ef} = 36 \times 10^{-40}$ cm^6/s and $R_C^{ef} = 19.3$ Å.

V. CONCLUSIONS

Based on our description of microscopic interaction between Er, Tm, and Ho(3+) ions in $LiYF_4$ crystals, several conclusions were derived to better understand the Ho-sensitization process in YLF crystals responsible for laser action at 2.1 μm. The $^5I_7$ active laser level of holmiun should be highly populated by an energy transfer from the first excited state of Er ions assisted by an energy migration throughout the $^4I_{13/2}$ levels because we found that $C_{\mathrm{Er-Er}} \approx 136.6 C_{\mathrm{Er-Ho}}$. In this case, the energy migration through $Er(^4I_{13/2})$ levels is a decisive mechanism for enhancing the energy transfer probability to $Ho(^5I_7)$ ions. When Tm ions work as donors, a competition between the $Tm(^3F_4) \rightarrow Ho(^5I_7)$ energy transfer and the migration of excitation through $^3F_4$ states is highly expected because of our observation that $C_{\mathrm{Tm\text{-}Tm}} \approx 2.4 C_{\mathrm{Tm\text{-}Ho}}$.

Both energy migrations through the $^4I_{13/2}(\mathrm{Er})$ and $^3F_4(\mathrm{Tm})$ excited levels play an important role for the $Ho(^5I_7)$ sensitization process in the Er:Tm:Ho:$LiYF_4$ laser crystal. Energy migration is an essential mechanism which must be taken into account in the case of $Ho(^5I_7)$ sensitization by Er.

The proposed approach for the overlap integral method, applied to the case of nonresonant energy transfer, has the advantage of being general and applicable to any donor-acceptor energy transfer involving $RE(3+)$ ions in solids. The microscopic parameters obtained using this method are not dependent on the employed statistic describing the interacting system. This was based on the overlap integral calculations using fundamental absorption and emission cross-section spectra. The proposed method constitutes a direct way of determining the critical radius of nonresonant energy transfer between $RE(3+)$ ions in solids. The non-vanishing overlap integral obtained using the spectrum shift of donor emission simulates the real case of using the emission sideband. This comment is also applicable to the overlap integral computed when involving the absorption sideband of an acceptor. Once having the critical radius value for the $(D \rightarrow A)$ energy transfer, it is possible to completely describe the energy-transfer efficiency of the system as a function of both D and A ion concentrations if the statistical distribution function between the involved ions is known.[12] This approach was recently employed to describe the energy-transfer processes in the Er:Tm:Ho:$LiYF_4$ crystal rods for a flash lamp pumping allowing the optimization of the dopant concentrations for a more efficient laser operation at 2.1 μm.[13]

ACKNOWLEDGMENTS

The authors would like to thank V. L. Salvador for the x-ray-fluorescence analysis allowing the concentration determination of RE ions in the samples. One of the authors, L. V. G. Tarelho, also thanks FAPESP for financial support. This work was financially supported by FINEP-PADCT, FAPESP, and CNPq.

*Electronic address: lgomes@net.ipen.br

[1] Z. Forster, Z. Naturforsch. B **49**, 321 (1949).
[2] D. L. Dexter, J. Chem. Phys. **21**, 836 (1952).
[3] T. Kushida, J. Phys. Soc. Jpn. **34**, 1318 (1973).
[4] S. A. Payne, L. K. Smith, W. L. Kway, J. B. Tassano, and W. F. Krupke, J. Phys.: Condens. Matter **4**, 8525 (1992).
[5] T. Miyakawa and D. L. Dexter, Phys. Rev. B **1**, 2961 (1970).
[6] F. Auzel and Y. H. Chen, J. Lumin. **66&67**, 224 (1995).
[7] F. Auzel, Phys. Rev. B **13**, 2809 (1976).
[8] F. Auzel and Y. Chen, J. Lumin. **65**, 45 (1995).
[9] D. E. McCumber, Phys. Rev. **136**, A954 (1964).
[10] G. M. Renfro, J. C. Windscheif, W. A. Sibley, and R. F. Belt, J. Lumin. **22**, 51 (1980).
[11] F. Auzel, in *Advances in Nonradiative Processes in Solids*, NATO ASI Series, Series B: Physics, Vol. 249, edited by Baldassare Di Bartolo (Plenum, New York, 1991).
[12] L. Gomes, L. C. Courrol, L. V. G. Tarelho, and I. M. Ranieri, Phys. Rev. B **54**, 3825 (1996).
[13] L. Gomes, L. V. G. Tarelho, L. C. Courrol, W. de Rossi, I. M. Ranieri, and S. P. Morato (unpublished).